

Beam steering based on coordinate transformation of Fermat spiral configurations

Cite as: AIP Advances 9, 075217 (2019); <https://doi.org/10.1063/1.5045489>

Submitted: 20 June 2018 . Accepted: 08 July 2019 . Published Online: 22 July 2019

G. Vasantharajan, N. Yogesh, and V. Subramanian 

COLLECTIONS

Paper published as part of the special topic on [Chemical Physics](#), [Energy, Fluids and Plasmas](#), [Materials Science](#) and [Mathematical Physics](#)



View Online



Export Citation



CrossMark

ARTICLES YOU MAY BE INTERESTED IN

[Broadband asymmetric transmission of linearly polarized electromagnetic waves based on chiral metamaterial](#)

Journal of Applied Physics **123**, 033103 (2018); <https://doi.org/10.1063/1.5008614>

[Acoustic focusing effect based on artificial periodic structure](#)

AIP Advances **9**, 075107 (2019); <https://doi.org/10.1063/1.5109603>

[Application of transformation optics in radar cross section reduction of targets with arbitrary two-dimensional geometries](#)

Journal of Applied Physics **125**, 234901 (2019); <https://doi.org/10.1063/1.5085289>



NEW: TOPIC ALERTS

Explore the latest discoveries in your field of research

SIGN UP TODAY!

Beam steering based on coordinate transformation of Fermat spiral configurations

Cite as: AIP Advances 9, 075217 (2019); doi: 10.1063/1.5045489

Submitted: 20 June 2018 • Accepted: 8 July 2019 •

Published Online: 22 July 2019



View Online



Export Citation



CrossMark

Vasantharajan G.,¹ Yogesh N.,² and V. Subramanian^{1,a)} 

AFFILIATIONS

¹Microwave Laboratory, Department of Physics, Indian Institute of Technology - Madras, Chennai 600036, India

²Department of Nuclear Physics, School of Physical Sciences, University of Madras, Guindy Campus, Chennai 600025, India

^{a)}Electronic mail: manianvs@iitm.ac.in

ABSTRACT

A two-dimensional transformational electromagnetic (T-E) device formed by configuring a circular disc with a Fermat spiral is realized. By tuning the phase of the emanating wave in the T-E medium, antenna switching and beam steering are made possible. To simplify the permittivity and permeability tensors of the proposed T-E device, a gradient index approach is employed using purely dielectric material, which is then realized using photonic crystals. The results are verified numerically using full wave simulations.

© 2019 Author(s). All article content, except where otherwise noted, is licensed under a Creative Commons Attribution (CC BY) license (<http://creativecommons.org/licenses/by/4.0/>). <https://doi.org/10.1063/1.5045489>

I. INTRODUCTION

Form invariance of Maxwell's equations under the coordinate transformation (CT) allows one to control electromagnetic (em) waves in unprecedented ways.¹⁻³ A CT from undistorted to distorted space (and vice versa) by means of geometrical operations such as rotation, reflection, stretching and squeezing can yield novel spatial profiles of dielectric permittivity, magnetic permeability and hence refractive index.^{4,5} Since an electromagnetic path follows the geodesics in any em medium, index profiles of transformed space provide greater degrees of freedom to mold the flow of light. For a decade, the scientific world clung with this branch of electromagnetics known as transformation electromagnetics (T-E), where resounding new devices such as invisibility cloak,^{2,3,6,7} em beam concentrator,⁸⁻¹⁰ collimator^{11,12} and flat lens^{13,14} have been continually proposed and some of them are realized subsequently. Though the tensors of the constitutive parameters of the transformed media are highly anisotropic and difficult to realize,^{15,16} the advent of metamaterial (MM)^{17,18} and photonic crystals (PhCs)^{19,20} serve as the potential candidates for the experimental realization of T-E devices.

The better known experimentally realized T-E based devices using MMs and PhCs are cloaks^{7,19,21} and lenses.^{11,22,23} Of which, lenses have wide range of applications and one such application is the antenna.¹⁵ It is found that using T-E based lenses, antennas with increased beam steering ability and high directivity can

be constructed.^{24,25} It is known that, even by increasing the number of elements in the phased array antenna (PAA),^{26,27} which is in the industrial use for a longer time, the directivity of PAA can be strengthened. However, for converting PAA into multiple-input multiple-output (MIMO) setup, the number of required elements would be huge and it can be impractical. Also there would be degradation of beam strength due to multi-directional output.²⁸ Moreover, the PAAs cannot steer the beam more than $\frac{2\pi}{3}$ radians.^{26,27} Currently MM-based²⁹ and PhC-based³⁰ PAAs are constructed to overcome the difficulties faced with PAAs. Nevertheless, the limitations of MM-based and PhC-based antennas are that, the device would work only at certain frequency range. Thus, still there is a scope for 2π radian beam steerer using T-E with high directivity and increased beam strength with slow field decay.

There are two ways of transformation electromagnetics approach by which highly collimated plane waves can be obtained and rotated. First, the highly collimated beam can be obtained by transforming the cylindrical wave into plane wave. By way of rotation¹⁵ the beam can be directed to the desired location. Secondly, by converting the cylindrical wave into a spiral wave, the wave can be rotated and be directed to the desired location. Since the second approach ensures minute control over beam steering angle, T-E device is constructed to mold the wave along spiral path. For the choice of spiral paths, one can consider any Archimedean spirals.

In this work, Fermat’s spiral is considered in order to have a slower variation of spirality with respect to angle ($r \propto \sqrt{\theta}$).

To transform the wavefront of a line source, that is, cylindrical waves, a cylindrical space (r, θ, z) is considered initially, which is then transformed into Fermat’s spiral space (r', θ', z') by CT. Due to the transformed coordinates, the em-wave emanating from line source propagate as Fermat’s spiral waves. The constitutive parameters (CPs) like relative permittivity ($\bar{\epsilon}'$) and relative permeability ($\bar{\mu}'$) of the transformed space can be derived⁶ as,

$$\bar{\epsilon}' = \frac{A\bar{\epsilon}A^T}{\det(A)} \quad \text{and} \quad \bar{\mu}' = \frac{A\bar{\mu}A^T}{\det(A)} \quad (1)$$

where, A and $\det(A)$ are the Jacobian matrix of the transformation and its determinant respectively. $\bar{\epsilon}$ and $\bar{\mu}$ are the relative permittivity and permeability of untransformed cylindrical space. By assigning the values of the space around the line source with $\bar{\epsilon}'$ and $\bar{\mu}'$, the cylindrical waves can be converted to Fermat spiral waves. Interestingly, by introducing complex coordinate transformation in Fermat’s spiral space, new space is obtained, where an em wave can be steered with novel electric field steering profiles.

The medium under test is placed at the center of the simulation environment which is a free space (air medium) truncated by perfectly matching layer boundary condition. A point source of 1 A/m, in this 2D simulation, is placed at the center of the medium under test. The time-harmonic electric field, E_z , of the em-wave due to the point source in Cartesian coordinates of u -space with amplitude E_0 , wave vector k and frequency ν is given by the equation,

$$E_z = E_0 e^{j\phi} \quad (2)$$

where

$$\phi = \vec{k} \cdot \vec{r} - \omega t, \quad k = \frac{\omega}{c}, \quad \omega = 2\pi\nu \quad (3)$$

Here, c is the speed of em-wave in vacuum and ϕ is the phase of the em-wave. The time-independent plane wave solution is analyzed in this article.

II. THEORY: FORMULATION OF FERMAT’S SPIRAL MEDIUM

To arrive at the circular wavefronts of a point source by CT, initially, u -space which is in the Cartesian system (Fig. 1a) representing physically isotropic medium, will be transformed to cylindrical coordinate system³¹ as in Fig. 1b. Thereby, obtaining a space that represents an em-wave with a radially directed electric field and circular wavefronts as in Eqs. (2), (4). The u -space in the cylindrical coordinate system is then transformed to v -space in the cylindrical coordinate system (Fig. 1c). Finally, the CT of v -space from the cylindrical coordinate system is transformed into the Cartesian coordinate system (Fig. 1d). Thus, the CTs which are to be performed to obtain the tensors of CPs, are in the order,

$$\begin{aligned} \text{CT - I} : u(x, y, z) &\rightarrow u(r, \theta, z) \\ \text{CT - II} : u(r, \theta, z) &\rightarrow v(r', \theta', z') \\ \text{CT - III} : v(r', \theta', z') &\rightarrow v(x', y', z') \end{aligned}$$

For the CT-I, the transformation equations are,

$$r = \sqrt{x^2 + y^2}, \quad \theta = \tan^{-1} \frac{y}{x}, \quad z = z; \quad (4)$$

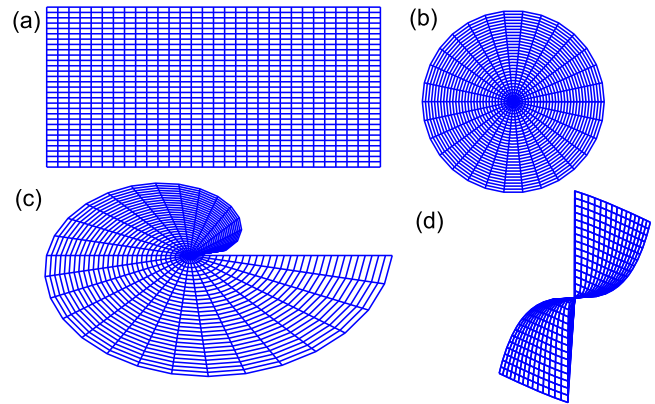


FIG. 1. (a) Untransformed Cartesian coordinate space $u(x, y, z)$, (b) Untransformed polar coordinate space $u(r, \theta, z)$, (c) transformed polar coordinate space $v(r', \theta', z')$ and (d) transformed Cartesian coordinate space $v(x', y', z')$.

The corresponding Jacobian matrix is,

$$A_1 = \frac{\partial(r, \theta, z)}{\partial(x, y, z)} = \begin{bmatrix} \frac{x}{r} & \frac{y}{r} & 0 \\ \frac{-y}{r^2} & \frac{x}{r^2} & 0 \\ 0 & 0 & 1 \end{bmatrix} \quad (5)$$

and the determinant is found to be,

$$\det(A_1) = \frac{1}{r} \quad (6)$$

The CPs representing the isotropic space¹⁰ $u(r, \theta, z)$ calculated using Eq. (1) are,

$$\bar{\epsilon} = \bar{\mu} = \begin{bmatrix} r & 0 & 0 \\ 0 & \frac{1}{r} & 0 \\ 0 & 0 & r \end{bmatrix} \quad (7)$$

Thus, the Cartesian coordinates of u -space are transformed into cylindrical coordinates of u -space. The circular geodesics represent the em-wavefront and the radial lines perpendicular to the circular geodesics represents the electric field direction in u -space.

Let R be the radius of the disc, then the range of r is from 0 to R . The angle is defined in the range $(-\pi, \pi]$. The angle varies continuously in the upper half plane as 0 to π and lower half plane of the disc as $-\pi$ to 0 respectively with branch points at π and $-\pi$. These are denoted in Fig. 2. As the principal argument of arctan is in the range $[-\frac{\pi}{2}, \frac{\pi}{2}]$, the value of θ (due to principal arguments of θ) in quadrants I and III is in the range $[0, \frac{\pi}{2}]$ and in quadrants II and IV is in the range $[-\frac{\pi}{2}, 0]$. This disc has to be transformed into v -space. To have a distinction between the untransformed and transformed spaces, they have been marked as unprimed and primed respectively.

Transforming the above obtained cylindrical space to Fermat’s spiral space ($r \rightarrow r\sqrt{\theta}$), the em-wavefront can be made from circular wave (as in Fig. 3a) into Fermat spiral as in Fig. 3b. Since this transformation do not depend on the radius of the disc, both r and r' are

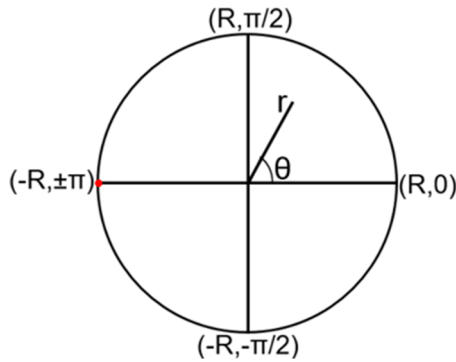


FIG. 2. The figure shows the disc of radius R . The upper half plane and the lower half plane of the disc have continuous variation of angle from 0 to π and $-\pi$ to 0 respectively. The red dot denotes the branch points π and $-\pi$. The field value at a point (r, θ) on the disc can be found out.

considered in the range 0 to R , here $R = 0.2$ m. Since the constituent parameters of v -space is proportional to the inverse of the metric^{32,33} of v -space, the transformation equations for CT II will be,

$$r' = \frac{r}{\sqrt{\theta}}, \quad \theta' = \theta, \quad z' = z; \quad (8)$$

The Jacobian matrix and its determinant of CT-II is,

$$A_2 = \frac{\partial(r', \theta', z')}{\partial(r, \theta, z)} = \begin{bmatrix} \frac{1}{\sqrt{\theta}} & \frac{-r}{2\sqrt{\theta^3}} & 0 \\ 0 & 1 & 0 \\ 0 & 0 & 1 \end{bmatrix} \quad (9)$$

and

$$\det(A_2) = \frac{1}{\sqrt{\theta}} \quad (10)$$

The CPs representing $v(r', \theta', z')$ calculated using Eq. (1) would be,

$$\vec{\epsilon}' = \vec{\mu}' = \begin{bmatrix} r' + \frac{r'}{4\theta'^2} & -\frac{1}{2\theta'} & 0 \\ -\frac{1}{2\theta'} & \frac{1}{r'} & 0 \\ 0 & 0 & r'\theta' \end{bmatrix} \quad (11)$$

Though the em-waves are transformed, space is represented in curved coordinates. The curved coordinates as such will have anisotropic permittivity and permeability tensors which are difficult

to realize practically. For this reason, if the transformed system is represented in Cartesian system the exact value of CPs at a given point can be obtained.⁴

Due to this aspect, CT-III is performed. The transformation equations, the Jacobian matrix and the determinant of the Jacobian matrix of CT-III are,

$$x' = r' \cos(\theta'), \quad y' = r' \sin(\theta'), \quad z' = z; \quad (12)$$

$$A_3 = \frac{\partial(x', y', z')}{\partial(r', \theta', z')} = \begin{bmatrix} \frac{x'}{r'} & -y' & 0 \\ \frac{y'}{r'} & x' & 0 \\ 0 & 0 & 1 \end{bmatrix} \quad (13)$$

and

$$\det(A_3) = r \quad (14)$$

The CPs representing $v(x', y', z')$ can be calculated using Eq. (1) is,

$$\vec{\epsilon}' = \vec{\mu}' = \begin{bmatrix} a_{11} & a_{12} & 0 \\ a_{12} & a_{22} & 0 \\ 0 & 0 & \theta' \end{bmatrix} \quad (15)$$

$$\begin{aligned} a_{11} &= 1 + \frac{\sin(2\theta')}{2\theta'} + \frac{\cos^2(\theta')}{4\theta'^2} \\ a_{12} &= \frac{-\cos(2\theta')}{2\theta'} + \frac{\sin(2\theta')}{8\theta'^2} \\ a_{22} &= 1 - \frac{\sin 2\theta'}{2\theta'} + \frac{\sin^2 \theta'}{4\theta'^2} \end{aligned} \quad (16)$$

The value of θ' , cosines and sines can be substituted using Eq. (10), that provides the value of CPs in terms of Cartesian coordinates. Also, it is to be noted that the value of permittivity of the medium along the polarisation direction (z -axis), (say) $\epsilon_{z'}$, is equal to θ' . As suggested by,^{4,33} the dielectric displacement of em-wave in v -space is found to be,

$$D_{z'} = \epsilon_0 \epsilon_{z'} E_{z'} = \epsilon_0 \theta' \left(\frac{\partial z}{\partial z'} \right) E_0 e^{j\phi'} = \epsilon_0 \theta E_0 e^{j\phi'} \quad (17)$$

where,

$$\phi' = kr - \omega t = kr' \sqrt{\theta'} - \omega t \quad \text{and} \quad \sqrt{\theta'} = \text{sgn}(y) \sqrt{\theta} \quad (18)$$

and ϵ_0 is the permittivity of free space.

From Eqs (4), (8) and (15), the value of $\epsilon_{z'}$ is equal to the principal values of angle (θ') of respective quadrants, which is shown

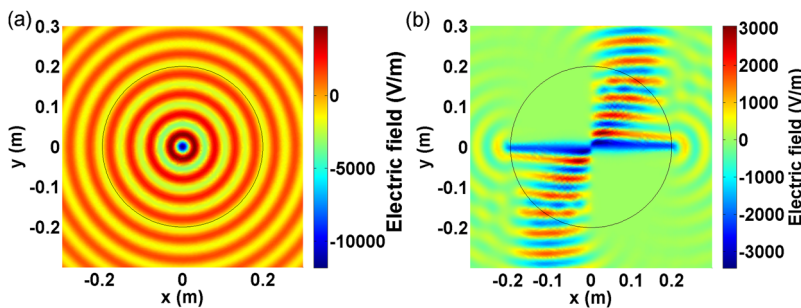


FIG. 3. The electric field map due to a point source at the centre of (a) u -space and (b) v -space.

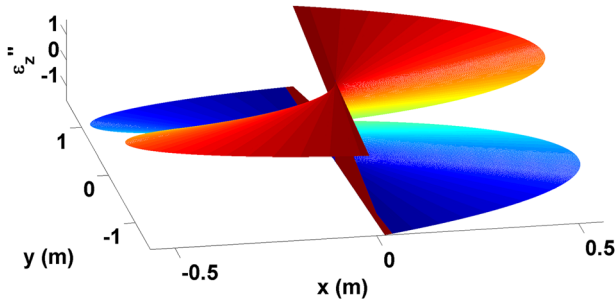


FIG. 4. ϵ_z'' represented in 3D.

in Fig. 4. The red regions (quadrants I and III) and blue regions (quadrants II and IV) indicate the positive and negative permittivity values respectively. There is a discontinuity in permittivity (also permeability) value at $x = 0$ line. These arguments can be obtained from Eqs (15) and (16). So, the em-wave from a quadrant of the disc is not allowed to propagate into the consecutive quadrants. Additionally, for the wave to propagate, the wave vector of the em-wave should be real. As already, k, r', ω and t are real, only positive values of θ could obtain real wave vector. Hence, for a point source placed at the center of the circular disk, the propagating em-wave will be directed along quadrants I and III as these quadrants are positive index (as given in Eq. (17)) and these allow only positive wave vectors (Eq. (18))³⁴ as shown in Fig. 3. This implies that, both, quadrants I and III are coupled. In order to couple the negative medium quadrants II and IV, the T-E medium has to be rotated.

III. COMPLEX TRANSFORMATION OF FERMAT SPIRAL SPACE

To understand the effect of change in the electromagnetic property of transformed medium due to its rotation, v -space is made to undergo complex transformation $r' \rightarrow r'' e^{jm\pi}$. In terms of Cartesian coordinate system, the transformation equations are,

$$x'' = x' e^{-jm\pi}, y'' = y' e^{-jm\pi}, z'' = z'; \quad (19)$$

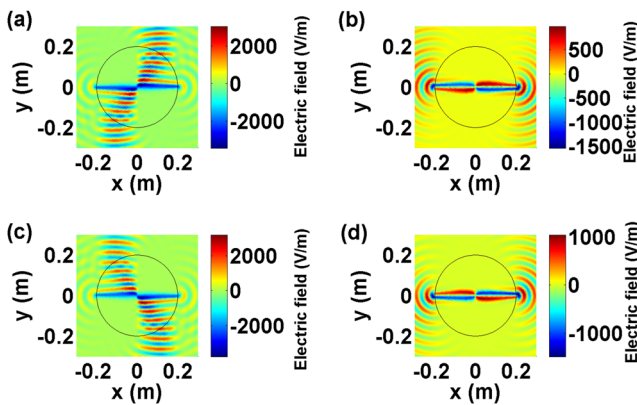


FIG. 5. Electric field map due to point source in w -space when, (a) $m = 0$ and 1, (b) $m = 0.25$, (c) $m = 0.5$ and (d) $m = 0.75$.

TABLE I. Value of ϕ'', θ' and nature of emanating wave for various m .

m	$\frac{\phi' + \omega t}{kr''}$	$\phi'' - \phi'$	θ'	Wave nature
0	$\sqrt{\theta''}$	0	$0 \leq \theta'' < \frac{\pi}{2}$	Propagate
0.25	$(\frac{1+j}{\sqrt{2}})\sqrt{\theta''}$	$\frac{\pi}{2}$	0	Decay
0.5	$j\sqrt{\theta''}$	π	$0 \geq \theta'' > \frac{-\pi}{2}$	Propagate
0.75	$(\frac{1-j}{\sqrt{2}})\sqrt{\theta''}$	$\frac{3\pi}{2}$	0	Decay
1	$-\sqrt{\theta''}$	2π	$0 \leq \theta'' < \frac{\pi}{2}$	Propagate

The value of CPs representing w -space are calculated using Eqs (1), (15) and (16),

$$\vec{\epsilon}'' = \vec{\mu}'' = \begin{bmatrix} a_{11} & a_{12} & 0 \\ a_{12} & a_{22} & 0 \\ 0 & 0 & \theta' e^{j2m\pi} \end{bmatrix} \quad (20)$$

Also, the dielectric displacement in vector form could be arrived using Eqs. (17–20),

$$\vec{D}_{z''} = \epsilon_0 \epsilon_{z''} E_{z''} \hat{z} = \epsilon_0 \theta' e^{j2m\pi} \left(\frac{\partial z'}{\partial z''} \right) E_0 e^{j\phi'} \hat{z} = \epsilon_0 \theta' E_0 e^{j\phi''} \hat{z} \quad (21)$$

where

$$\phi'' = \phi' + 2m\pi = kr'' \sqrt{\theta'} e^{jm\pi} - \omega t + 2m\pi \quad (22)$$

and \hat{z} is the unit vector of z -axis, indicating the em-wave polarisation direction.

Eqs. (19–22) implies that the real space is transformed to complex space by CT. Let this complex space be w -space. It is a well-known fact that, as m changes, the change in the value of $e^{jm\pi}$ in Eq. (19) represents the anti-clockwise rotation of the planes of w -space. This is reflected in the permittivity of the em-wave, as $\epsilon_{z''} \propto e^{j2m\pi}$. In fact, for $m = 0$ and 1, the value of $\epsilon_{z''}$ is the same (shown in Fig. 5a). Remarkably, for every anti-clockwise half-rotation of w -space, the medium gets rotated fully in the anti-clockwise direction. Therefore, the value of m is within the range 0 to 1, can be discussed since the rest (for any real number m) would be similar. The electric field map for $m = 0.25, 0.5$ and 0.75 are also

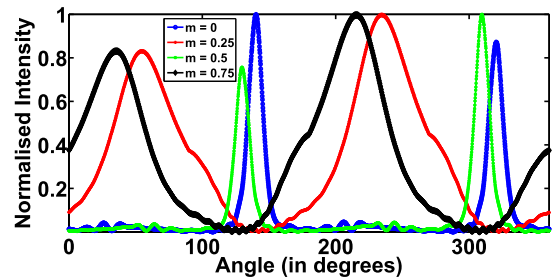


FIG. 6. Normalised intensity profile at 6 GHz.

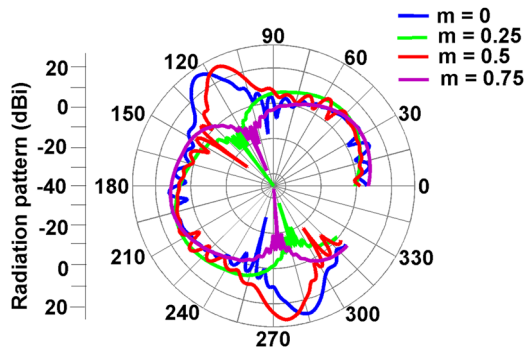


FIG. 7. Radiation pattern of the disc at 6 GHz for the source kept at the center. Angle, in degrees, are given at the circumference of the polar plot.

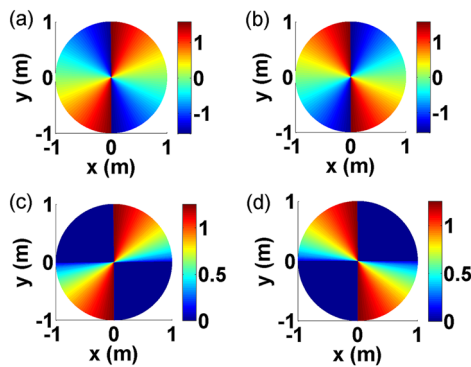


FIG. 8. The value of ϵ_z for GRIN disc obtained from T-E medium (w -space) for (a) $m = 0$, (b) $m = 0.5$, and $n_G = \text{Re}(\sqrt{\epsilon_z})$ for (c) $m = 0$, (d) $m = 0.5$.

plotted as Fig. (5b), (5c) and (5d). For $m = 0, 0.5$ and 1 , the propagating planar wave emanates from the T-E medium while for $m = 0.25$ and 0.75 , the decaying field emanates from the T-E medium. The values of ϕ'' , possible values of θ' , the respective D_z'' and the nature of emanating wave are presented in Table I.

Now, experimentally, to tune the phase of the em-wave emanating from the T-E medium, the T-E medium could be rotated or incorporate suitable functional reconfigurable materials (FRMs) such as liquid crystals (a function of temperature) and ferrites (a function of magnetic field)³⁵ as fixed T-E medium. Other possible rotator configurations would be the combination of both these methods.

To perceive the tuning of the phase by physically rotating the T-E medium, a thought experiment could be considered. Let, the disc-shaped 3D T-E medium can be thought of having a dimension (l) along z -axis such that $l^2 < R^2$. Initially, the em-wave is polarised along the z -axis for $m = 0$ case, for $m = 0.25$, from Eqs. (21 and 22), in real space, the disc is first rotated anti-clockwise along the x -axis by $\frac{\pi}{2}$ radians and then undergo one more anti-clockwise rotation along the y -axis by $\frac{\pi}{2}$ radians. Consequently, the z -polarised em-wave emanating out of x -axis (or $y = 0$ line) is a decaying field as in Fig. 5b. Similarly, for $m = 0.5$, in real space, from the initial state of the disc, the disc undergoes anti-clockwise rotation along the x -axis as well as y -axis by π radians, resulting in an inverted disc. So, the z -polarised em-wave emanates out of y -axis as shown in Fig. 5c. Precisely, the change in the value of m mathematically denotes physical rotations.

The intensity profile and the radiation pattern of the emanating em-wave computed at a distance 10 times the wavelength (λ) considered will be as in Fig. 6 and Fig. 7. These figures indicate that, the beam is more directional and intense for $m = 0, 0.5$ and 1 , acting like a bi-directional antenna and for $m = 0.25$ and 0.75 , the radiation pattern is similar to that of a classical dipole antenna. Once the desired radiation pattern is achieved, the disc can be rotated along the z -axis to steer the beam in any direction. As an example, for $m = 0$, if the disc is rotated along the z -axis, the peak directivity can be shifted to any desired angle without any change of phase or polarisation. Thus, using the proposed T-E medium the em-wave can be steered in the desired direction with the desired radiation pattern by switching to the desired antenna mode. Hence, the proposed T-E medium can be used for beam steering and antenna switching.

IV. GRIN MEDIUM

Realizing such a medium (or material) with same tensors of ϵ_r and μ_r is practically impossible. To overcome this, one can construct gradient index medium (GRIN) with respect to the polarization state of a given em-wave. Since the proposed T-E device works under TE polarization, ϵ_z (the primes are dropped hereafter) may be sufficient enough to observe the similar effect for TE excitation. Consequently, GRIN disc is designed entirely with a dielectric medium using ϵ_z of the T-E disc in order to maintain it as a nonmagnetic material (refer Eq. (23)). The refractive index of the GRIN media that mimics w -space is,

$$n_G = \text{Re}(\sqrt{\epsilon_z}) = \text{Re}(\sqrt{\theta} e^{jm\pi}) \tag{23}$$

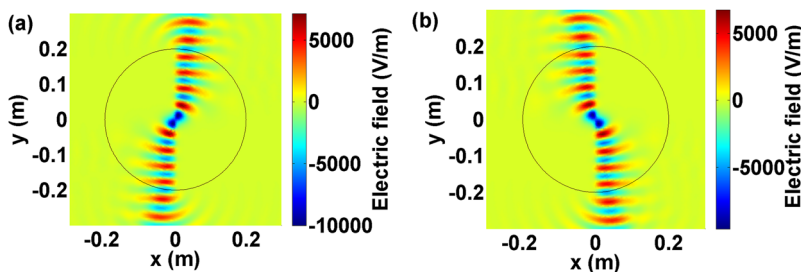


FIG. 9. E_z field maps for a GRIN disc that mimics T-E w -space with m values, (a) 0 and (b) 0.5.

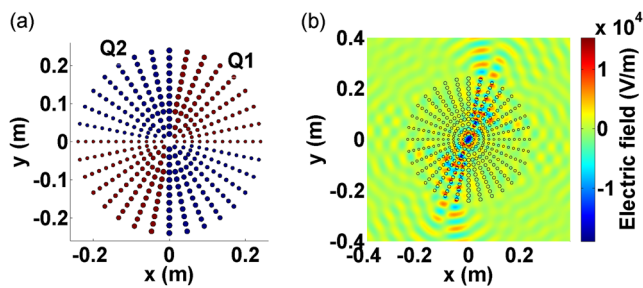


FIG. 10. (a) Beam Steerer made of photonic crystal made up of materials with dielectric constants 9(Q1) and 4.2(Q2). (b) Electric field map at 5.58 GHz.

The allowed value of, both, $\sqrt{\theta}$ and $e^{jm\pi}$ are purely real and purely imaginary for m values 0 and 0.5 respectively. Eventually, the value of n_G for m values 0 and 0.5 are positive and negative respectively. The permittivity profile and refractive index profile for GRIN disc are given in Fig. 8 for m values 0 and 0.5. The index profiles explain why em-wave is steered in specific quadrants for $m = 0$ and $m = 0.5$, as e-m wave will be confined along the high index regime. By repeating the e-m simulation for a GRIN disc, it is found that GRIN disc acts similarly to the T-E based disc but the dispersion of the wave is high in GRIN disc than in T-E device as shown in Fig. 9. Thus the simplified GRIN system ensures the beam steering ability of the proposed T-E device.

V. REALISATION USING PHOTONIC CRYSTAL (PhC)

While the design of GRIN disc eliminates the requirement of permeability tensor, realizing a continuous spatial profile of dielectric permittivity also poses a challenge for practical realization. In fact using PhCs and MMs, one can have higher feasibility to obtain smooth spatial variation of dielectric values within the geometrical optics limit. The device proposed in PhC can be scaled to any other frequency. So, the GRIN PhC is chosen over MM. The GRIN PhC is made up of four wedges, where similar wedges occupy opposite quadrants. Wedge Q1 (red colour) and Q2 (blue colour) are placed in odd quadrants (I and III) and even quadrants (II and IV) respectively. Wedges Q1 and Q2 are made up of circular rods of permittivity 9 (Alumina) and 4.2 (Quartz glass) with a varying diameter as shown in Fig. 10a. The arrangement provides a varying refractive index for the photonic crystal system to steer the beam along Fermat spiral. The lattice constant (a) of the GRIN PhC is 2 cm and radii of rods vary from $0.2a$ to $0.4a$ linearly at an interval $a/40$. Fig. 10b provides the electric field profile for a point source placed at the centre of the geometry. The dispersion of the em-wave in GRIN PhC is similar to GRIN medium in the Section IV.

VI. CONCLUSION

In summary, a Fermat spiral transformation based T-E device (disc-shaped) is constructed. It is shown that, by tuning the phase velocity, the em-wave can be steered and the desired radiation pattern can be achieved in the desired direction. Thus, the proposed device can be used for beam steering and antenna switching.

The proposed device is impedance matched medium with air, as tensors of permittivity and permeability are the same. As the medium depends on polarisation state, to realize the medium practically, an all dielectric GRIN based medium having the refractive index equal to that of the square root of z-component of the dielectric permittivity of the T-E medium is proposed. The GRIN medium performs beam steering very similar to the proposed T-E medium, but the dispersion in the medium is higher than the proposed T-E medium. The GRIN disc is reconstructed using photonic crystals for the realization of proposed beam steering disc. Owing to the need for miniaturized beam steering applications in THz and optical communication, the proposed transformation electromagnetics based device is anticipated as one of the novel candidates as it can steer the beam in a specific direction with high directivity and increased beam strength with slow field decay, and for antenna switching.

REFERENCES

- 1 A. Ward and J. B. Pendry, "Refraction and geometry in Maxwell's equations," *Journal of Modern Optics* **43**, 773–793 (1996).
- 2 J. B. Pendry, D. Schurig, and D. R. Smith, "Controlling electromagnetic fields," *Science* **312**, 1780–1782 (2006).
- 3 U. Leonhardt, "Optical conformal mapping," *Science* **312**, 1777–1780 (2006).
- 4 U. Leonhardt and T. G. Philbin, "Transformation optics and the geometry of light," in *Progress in Optics*, Vol. 53 (Elsevier, 2009) pp. 69–152.
- 5 J. Pendry, Y. Luo, and R. Zhao, "Transforming the optical landscape," *Science* **348**, 521–524 (2015).
- 6 D. Schurig, J. Pendry, and D. R. Smith, "Calculation of material properties and ray tracing in transformation media," *Optics Express* **14**, 9794–9804 (2006).
- 7 R. Liu, C. Ji, J. Mock, J. Chin, T. Cui, and D. Smith, "Broadband ground-plane cloak," *Science* **323**, 366–369 (2009).
- 8 M. Rahm, D. Roberts, J. Pendry, and D. Smith, "Transformation-optical design of adaptive beam bends and beam expanders," *Optics Express* **16**, 11555–11567 (2008).
- 9 W. Wang, L. Lin, J. Ma, C. Wang, J. Cui, C. Du, and X. Luo, "Electromagnetic concentrators with reduced material parameters based on coordinate transformation," *Optics Express* **16**, 11431–11437 (2008).
- 10 J. Yang, M. Huang, C. Yang, Z. Xiao, and J. Peng, "Metamaterial electromagnetic concentrators with arbitrary geometries," *Optics Express* **17**, 19656–19661 (2009).
- 11 D.-H. Kwon and D. H. Werner, "Transformation optical designs for wave collimators, flat lenses and right-angle bends," *New Journal of Physics* **10**, 115023 (2008).
- 12 K. Yao, X. Jiang, and H. Chen, "Collimating lenses from non-Euclidean transformation optics," *New Journal of Physics* **14**, 023011 (2012).
- 13 D.-H. Kwon and D. H. Werner, "Beam scanning using flat transformation electromagnetic focusing lenses," *IEEE Antennas and Wireless Propagation Letters* **8**, 1115–1118 (2009).
- 14 C. Mateo-Segura, A. Dyke, H. Dyke, S. Haq, and Y. Hao, "Flat Luneburg lens via transformation optics for directive antenna applications," *IEEE Transactions on Antennas and Propagation* **62**, 1945–1953 (2014).
- 15 D. H. Werner and D.-H. Kwon, *Transformation electromagnetics and metamaterials* (Springer, 2015).
- 16 Y. A. Urzhumov, N. B. Kundtz, D. R. Smith, and J. B. Pendry, "Cross-section comparisons of cloaks designed by transformation optical and optical conformal mapping approaches," *Journal of Optics* **13**, 024002 (2010).
- 17 W. Tang, C. Argyropoulos, E. Kallou, W. Song, and Y. Hao, "Discrete coordinate transformation for designing all-dielectric flat antennas," *IEEE Transactions on Antennas and Propagation* **58**, 3795–3804 (2010).
- 18 X. Wu, P.-H. Tichit, S. N. Burokur, S. Kirouane, A. Sellier, and A. de Lustrac, "Numerical and experimental demonstration of a coordinate transformation-based azimuthal directive emission," *Microwave and Optical Technology Letters* **54**, 2536–2540 (2012).

- ¹⁹N. Yogesh and V. Subramanian, "Directional cloak formed by photonic crystal waveguides," in *Microwave Symposium Digest (MTT), 2012 IEEE MTT-S International* (IEEE, 2012) pp. 1–3.
- ²⁰Y. Cao, J. Xie, Y. Liu, and Z. Liu, "Modeling and optimization of photonic crystal devices based on transformation optics method," *Optics Express* **22**, 2725–2734 (2014).
- ²¹D. Schurig, J. Mock, B. Justice, S. A. Cummer, J. B. Pendry, A. Starr, and D. Smith, "Metamaterial electromagnetic cloak at microwave frequencies," *Science* **314**, 977–980 (2006).
- ²²D. Roberts, N. Kundtz, and D. Smith, "Optical lens compression via transformation optics," *Optics Express* **17**, 16535–16542 (2009).
- ²³D. Lu and Z. Liu, "Hyperlenses and metalenses for far-field super-resolution imaging," *Nature Communications* **3**, 1205 (2012).
- ²⁴J. Gao, C. Wang, K. Zhang, Y. Hao, and Q. Wu, "Beam steering performance of compressed Luneburg lens based on transformation optics," *Results in Physics* **9**, 570 (2018).
- ²⁵A. Boriskin and R. Sauleau, *Aperture Antennas for Millimeter and Sub-Millimeter Wave Applications* (Springer, 2017).
- ²⁶A. Fenn, *Adaptive Antennas and Phased Arrays for Radar and Communications*, Antennas (Artech House, 2007).
- ²⁷J. M. Robert, *Phased Array Antenna Handbook* (Artech House, 2017).
- ²⁸W. Hong, Z. H. Jiang, S. He, J. Zhou, P. Chen, Z. Yu, J. Chen, L. Tian, C. Yu, J. Zhai *et al.*, "Limitations of phased arrays for 5g wireless communications," in *Antennas and Propagation & USNC/URSI National Radio Science Meeting, 2017 IEEE International Symposium on* (IEEE, 2017) pp. 1467–1468.
- ²⁹Y. Liu, X. Jin, X. Zhou, Y. Luo, K. Song, L. Huang, and X. Zhao, "A phased array antenna with a broadly steerable beam based on a low-loss metasurface lens," *Journal of Physics D: Applied Physics* **49**, 405304 (2016).
- ³⁰J. Lei, J. Yang, X. Chen, Z. Zhang, G. Fu, and Y. Hao, "Experimental demonstration of conformal phased array antenna via transformation optics," *Scientific Reports* **8**, 3807 (2018).
- ³¹M. Rahm, D. Schurig, D. A. Roberts, S. A. Cummer, D. R. Smith, and J. B. Pendry, "Design of electromagnetic cloaks and concentrators using form-invariant coordinate transformations of Maxwell's equations," *Photonics and Nanostructures-Fundamentals and Applications* **6**, 87–95 (2008).
- ³²R. A. Crudo and J. G. O'Brien, "Metric approach to transformation optics," *Physical Review A* **80**, 033824 (2009).
- ³³L. Bergamin, P. Alitalo, and S. Tretyakov, "Nonlinear transformation optics and engineering of the Kerr effect," *Physical Review B* **84**, 205103 (2011).
- ³⁴J. Skaar, "On resolving the refractive index and the wave vector," *Optics Letters* **31**, 3372–3374 (2006).
- ³⁵P. Grant, F. Castles, Q. Lei, Y. Wang, J. Janurudin, D. Isakov, S. Speller, C. Dancer, and C. Grovenor, "Manufacture of electrical and magnetic graded and anisotropic materials for novel manipulations of microwaves," *Phil. Trans. R. Soc. A* **373**, 20140353 (2015).